

PAPER • OPEN ACCESS

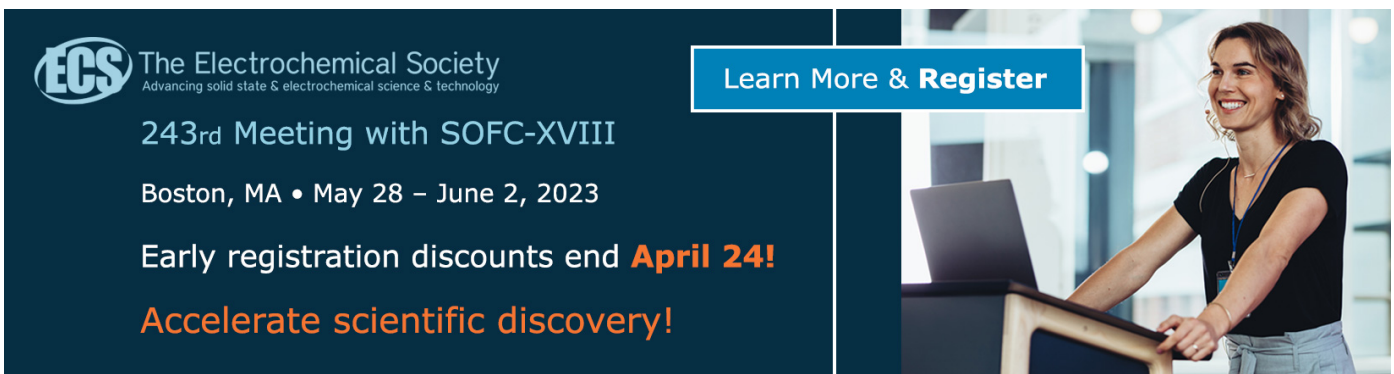
Rapid solidification during welding of duplex stainless steels – in situ measurement of the chemical concentration by Laser-Induced Breakdown Spectroscopy (LIBS)

To cite this article: L Quackatz *et al* 2023 *IOP Conf. Ser.: Mater. Sci. Eng.* **1274** 012018

View the [article online](#) for updates and enhancements.

You may also like

- [Study on Welding Process of 7x0.5 Multilayer 304 Bellows and Flange](#)
Zhaodong Jiang, Dong Liang, Tong Zhou et al.
- [Analysis of Laser-Induced Plume During Disk Laser Welding at Different Speeds](#)
Teng Wang, , Xiangdong Gao et al.
- [Measurement of the composition change in Al5754 alloy during long pulsed Nd : YAG laser welding based on LIBS](#)
M Jandaghi, P Parvin, M J Torkamany et al.



ECS The Electrochemical Society
Advancing solid state & electrochemical science & technology


243rd Meeting with SOFC-XVIII

Boston, MA • May 28 – June 2, 2023

Early registration discounts end **April 24!**

Accelerate scientific discovery!

Learn More & Register



Rapid solidification during welding of duplex stainless steels – in situ measurement of the chemical concentration by Laser-Induced Breakdown Spectroscopy (LIBS)

L Quackatz¹, A Griesche¹ and T Kannengiesser^{1,2}

¹ Federal Institute for Materials Research and Testing, Unter den Eichen 87, Berlin 12205, Germany

² Otto-von-Guericke University Magdeburg, Faculty of Mechanical Engineering, Institute of Materials and Joining Technology, Universitätsplatz 2, 39106 Magdeburg, Germany

Lukas.quackatz@bam.de

Abstract. Duplex stainless steels (DSS) are frequently used, especially in applications requiring high strength combined with high corrosion resistance in aggressive media. Examples include power plant components and maritime structures. During welding of these steels, local variations in chemical composition can occur. This results in ferritization of the material and negatively affects the mechanical properties of the components. In this work, tungsten inert gas (TIG) welding experiments were performed with DSS. Chemical composition analysis was realized in situ by using Laser Induced Breakdown Spectroscopy (LIBS). The aim of the work is to quantitatively measure the chemical composition in the weld seam of various DSS and to identify possible influences of welding parameters on the microstructure of the material. The chemical concentrations of the main alloying elements Cr, Ni, Mn on the surface of the sample during the welding process and the cooling process were measured. Mn and Ni are austenite stabilizers and their content increases during welding by using certain high alloyed filler material. Spectra were recorded every 1.3 s at a spacing of approximately 2 mm. During the cooling process the location of the measurement was not changed. The LIBS method is proved to be suitable for the quantitative representation of the chemical compositions during the welding process.

1. Introduction

The microstructure of duplex stainless steels (DSS) is characterized by a balanced ratio of austenite (γ) and ferrite (α). Austenite is embedded in the ferrite matrix. The suppression of the formation of martensite is due to the high proportions of alloying elements. With the high proportion of α -stabilizing elements such as Cr, Mo and additionally a low proportion of γ -stabilizing elements such as Ni, Mn, N, a ferritic-austenitic matrix is formed. The advantages of both phases are combined [1, 2]. Most DSS welds solidify completely ferritic. Dendrite growth follows the temperature gradient and a coarse-grained ferrite matrix results. The solid-state transformation of $\alpha \rightarrow \alpha+\gamma$ is diffusion-driven and thus time-dependent. Austenite precipitates as inter- and intragranular phase [1]. To achieve a balanced phase ratio in the microstructure of the DSS, workpieces are solution annealed ($> 1,000^\circ\text{C}$) and quenched subsequently. In this way, the required microstructure originates and excellent mechanical properties of the DSS can be adjusted and utilized. Many industrial applications require a welding process and due to uncontrolled, rapid cooling and loss of alloying elements an unbalanced γ to α ratio can originate, resulting in low corrosion resistance, low ductility and solidification cracking susceptibility. Furthermore, too slow cooling can lead to precipitation of intermetallic phases. Particularly worthy to mention are chromium nitrides and carbides [3-5]. Recommendations for



welding duplex steels are given in [6] and mainly relate to the heat input during welding, the chemical composition of the molten pool and the design of the weld.

Even the slightest element burnup during the welding process can lead to the critical change of the chemical composition and ferritization of the weld metal. Yang et al. [7] have shown that an unbalanced γ/α ratio with 80-90 % α in the weld metal (EN grade 1.4462) causes significant cracking problems in safety critical components. Martin et al. [8] have shown that the high temperature fracture strength of DSS increases dramatically with increasing γ -volume fraction. In order to predict the phase ratio of duplex steels after welding, some diagrams (Schaeffler, De Long and WRC1992) exist with which the microstructure in the weld metal, based on Cr_{eq} and Ni_{eq} can be calculated [9-11]. Recent research has shown that the calculation of Cr_{eq} and Ni_{eq} is inaccurate and needs adjustments [12, 13].

The aforementioned problems in welding duplex steels underscore the need for an in situ measurement method to predict the weld microstructure. Currently developed examination methods for welded components either inadequately predict the resulting solidification modes and ferrite contents of the welds or use post-mortem, destructive examination methods such as metallographic determination. Laser Induced Breakdown spectroscopy (LIBS) provides a highly accurate, effectively non-destructive, time- and spatially resolved quantitative measurement of chemical composition during welding, i.e., before, during, and after solidification of the weld metal in the fusion zone (FZ) and heat-affected zone (HAZ). In addition, the results from LIBS measurements can predict spatially resolved, localized buildup. LIBS is a spectroscopic technique based on the element-specific photon emissions of the plasma. A high-energy, pulsed laser is focused on the surface, of the sample under investigation and locally introduces heat into the material. The material begins to evaporate and a microplasma is formed. During the cooling of the plasma, element-specific radiation is produced, which can be evaluated with help of a spectrometer and suitable software. If the measurement method is calibrated, quantitative analyses can also be performed [14].

A common welding process is tungsten inert gas (TIG) welding. An arc is generated between a tungsten electrode and the workpiece by means of a sufficiently high current. A shielding gas (usually Ar) is used to prevent oxidation of the workpiece and electrode. The high heat flux of the welding plasma melts the workpiece and creates a weld pool. Vaporization of the molten material can release metal vapor from the surface of the weld pool. If the loss of material results in a critical change in chemical composition, the microstructure of the material can be altered and the mechanical properties of the weld can be affected. The complex processes of burning-off of alloying elements can be found in relevant literature and will not be described further here [15, 16].

LIBS could already be used as a suitable method for monitoring the weld pool chemistry as done by Taparli et al. [17]. Of particular interest was the detection of burnt manganese from the weld pool dejected on the HAZ of austenitic steels [18]. Previous research was able to demonstrate the feasibility of in situ measurement, as well as quantitative analysis of welded duplex steels and will now be further validated in this work. Furthermore, LIBS results could be validated with conventional EDS measurements [19]. With the help of an enhanced multivariate calibration, the quantitative analysis becomes more precise and reliable. The chemical composition of the weld pool can now be monitored using LIBS.

2. Materials and methods

2.1. Materials

Two different duplex steels (EN grade 1.4462 and 1.4162) were investigated in this research. Table 1 lists the chemical compositions of the sample materials and the filler metal. The chemical composition was measured with a conventional spark emission spectroscopy instrument from SPECTRO Analytical Instrument GmbH.

Table 1. Selected sample materials and their chemical compositions (measured with Spark-OES).

Grade (EN 10088-1)	Chemical Composition (wt. %)						
	C	Si	Mn	Cr	Ni	Mo	Fe
1.4462	0.020	0.320	1.680	22.650	5.790	2.970	Bal.
1.4162	0.018	0.600	4.950	21.940	1.540	0.310	Bal.
AWS ER 347 ^a	0.020	0.960	1.170	18.81	9.770	0.060	Bal.

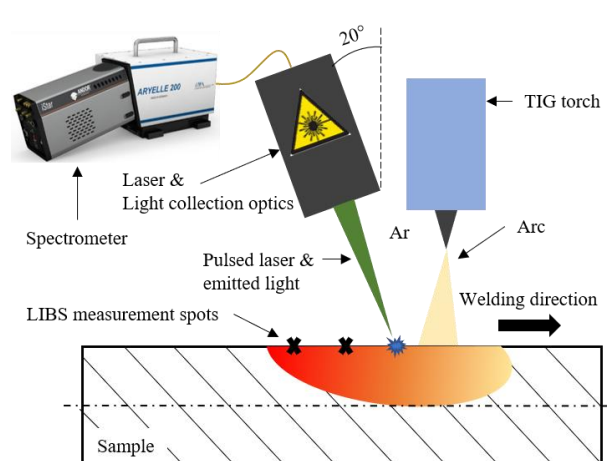
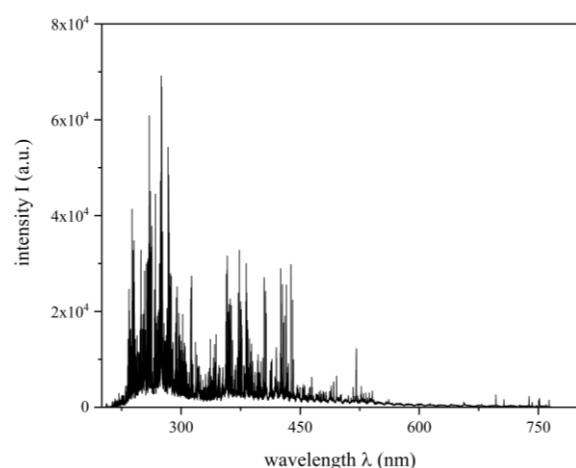
^a filler material EN ISO 14343-A

Flat specimens, measuring 150 x 35 x 5 mm³ (length x width x thickness) were fabricated for the experiments. Before welding experiments were carried out, the specimens were cleaned with acetone to remove contamination from production and processing.

2.2. Experimental

The welding experiments were carried out with the tungsten inert gas (TIG) welder CastoTIG 1611 DC power supply, from the company Castolin. A pure tungsten electrode, with a diameter of 1.6 mm, was used. All welding experiments were performed with an Ar shielding gas flow of 10 L/min. The electrode had a distance of 3 mm to the workpiece and the gas nozzle has a diameter of 6 mm. With the help of a linear motor, the specimens were welded at a constant speed.

The LIBS system includes a pulsed 1064 nm Nd:YAG laser, with a 15 Hz pulse rate and a maximum pulse energy of 200 mJ (Quantel CFR 200). The laser was synchronized with an Echelle spectrometer (Aryelle 200) from LTB Lasertechnik Berlin GmbH using a LIBS controller. To achieve the maximum time resolution, the spectrometer is connected to an Andor iStar ICCD detector from Oxford Instruments [20]. In figure 1 the experimental setup can be seen. The laser head is tilted by 20°, relative to the surface normal, so that the laser measurement spot can be focused 10 mm from the welding arc on the surface of the sample. Information is hardly lost due to this inclination. A light collecting optics (focal length: 300 mm) was used to focus the laser beam on the surface of the specimen. Subsequently, the electromagnetic radiation was collected with an optical fiber (same system) with a focal length of 10 mm and directed into the spectrometer. Due to the additional electromagnetic radiation from the welding plasma, additional optical filters are built into the LIBS system. For all experiments, the gate width was 40 μs and the delay time was 1 μs. These configurations were found to be promising in previously performed experiments [19]. For one spectrum 15 laser shots were accumulated.

**Figure 1.** Sketch of the experimental set-up.**Figure 2.** LIBS Spectrum of a Duplex stainless steel EN grade 1.4162.

The duplex steel specimens were welded at a constant welding speed of 10 cm/min and welding currents of 140 A and 160 A, respectively. Welding was performed both with and without filler metal. The total length of the welds was 50 mm. After the laser was started and spectra were recorded, the Ar

shielding gas supply started after about 3 s. The welding arc then ignited and the linear motor started until the final length of 50 mm was reached. The welding arc was switched off and the shielding gas switched off after approx. 3 s. The LIBS laser was turned off after the specimen reached a surface temperature of 150°C. The surface temperature in the weld pool was measured using a non-contact laser pyrometer from Advanced Energy. The LIBS measuring spots were always recorded directly (10 mm) behind the welding torch. Accordingly, the measuring spots are initially in the base material, during welding in the molten material and at the end of the welding process in the solidified weld metal. The in situ LIBS spectra were recorded in the spectral range of 200 – 800 nm. The background noise in the recorded spectra was removed using the software AirPls [21].

3. Results and discussion

The solidified, cooling and molten material were recorded with the same configurations. Figure 2 shows a LIBS spectrum of a DSS EN grade 1.4162 with the corresponding spectral range.

In general, the overall goal of most chemical measurement methods is to produce a quantitative measurement with the highest possible precision. A considerable amount of literature has been published on calibration methods and procedures [22, 23]. Experimental calibrations are performed by measuring a series of calibration samples containing the analyte (or analytes) of interest in sensibly graded amounts. Materials whose contents are known with the greatest possible reliability are used as calibration samples. The contents of these calibration samples can be considered to be free of errors compared to the measurement results. The advantage of LIBS is that little preparation is required to measure the samples. For a quantitative measurement, calibration curves must be prepared in advance. A distinction is made between univariate and multivariate calibration. Multivariate models are usually associated with a higher computational and model building effort, such as the Partial Least Squares (PLS) method [22]. In previous work [19], simple univariate models were used for quantification. Now, the calibration using the PLS method, has been optimized and provides reliable results. For calibration, 30 certified reference materials were used. The calibration was validated in this work.

3.1. *In situ measurements of element concentration during TIG welding*

The welding tests were carried out both with and without filler material. Compared here are the experiments of two different grades of duplex steels (EN grade 1.4462 and 1.4162) with two different amperages (160 A and 140 A). The welding speed was kept constant at 10 cm/min. Figure 3 shows the results of the quantitative analysis of the in situ LIBS measurement during welding. The timing of the welding process can be read directly from the diagram. At $t = 4$ s, the welding torch started and there is a brief increase in concentration due to the flashing of the plasma and the additional electromagnetic radiation picked up by the spectrometer. This phenomenon has been explained in previous research [19]. The concentrations of Mn increase sharply during welding. However, the concentration of Ni remains mostly constant. Mn can burn off during welding due to its low enthalpy of vaporization (220 kJ/mol). Ni has a much higher enthalpy of vaporization (372 kJ/mol) and therefore does not burn off [24]. The burned-off Mn is detected by the LIBS measurement and is therefore elevated [25]. After the welding process ($t \sim 30$ s), the concentrations drop. Then the cooling process of the samples down to 150°C starts. Table 2 shows the mean values of the chemical compositions in the weld metal during the cooling process of the main alloying elements (evaluated with PLS). It is striking that the Ni concentrations increase in all welds with filler metal. In contrast, the Mn concentrations increase only with a welding current of 140 A and the use of the filler metal. The Cr concentrations are inconspicuous and predominantly stable.

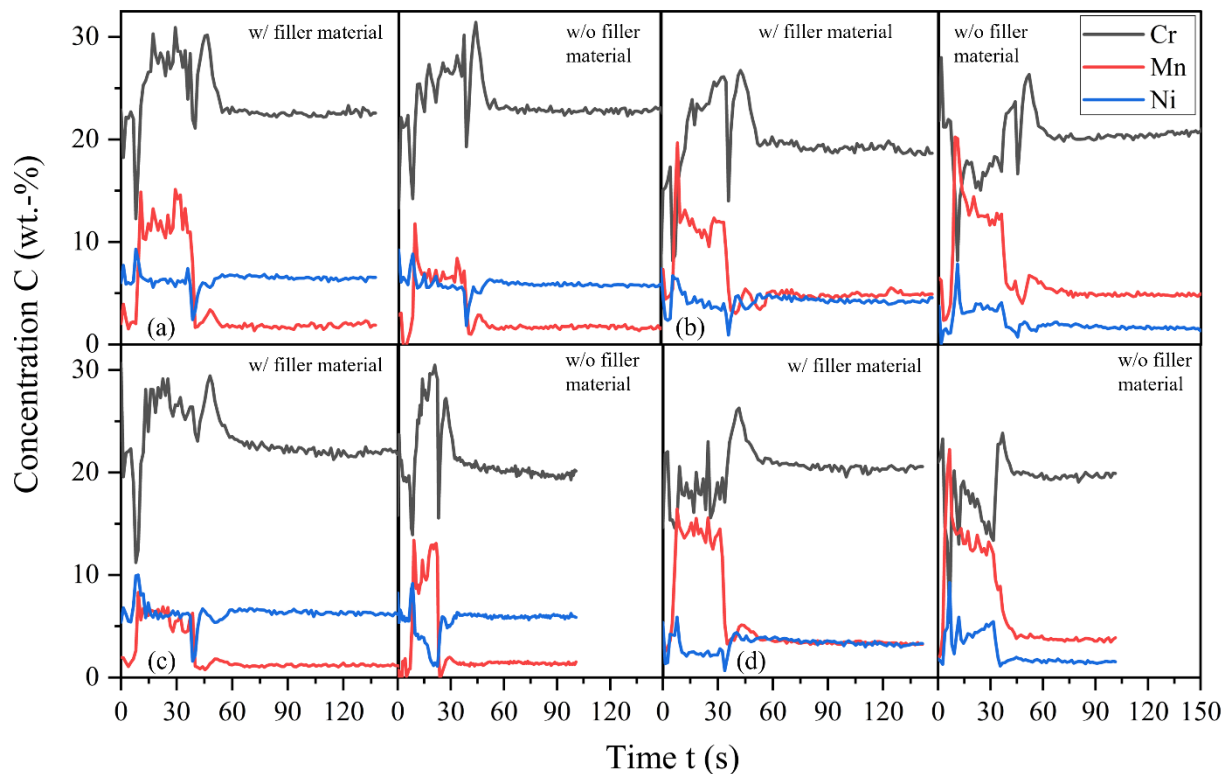


Figure 3. In situ measurement of chemical composition during TIG welding of duplex steels with and without filler material. Representation of the main alloying elements Cr, Ni and Mn. (a) EN grade 1.4462 140 A; (b) EN grade 1.4162 140 A; (c) EN grade 1.4462 160 A; (d) EN grade 1.4162 160 A.

Table 2: PLS quantification of the weld material after welding process with different current levels, both with and without filler metal. Mean values of the chemical concentrations of the main alloying elements.

Alloying element	Chemical Composition (wt.-%)			
	EN grade 1.4162			
	140 A		160 A	
	With filler material	Without filler material	With filler material	Without filler material
Cr	19.3	20.0	20.4	19.7
Ni	4.2	1.7	3.5	1.6
Mn	5.0	4.9	3.5	3.8

Alloying element	EN grade 1.4462			
	140 A		160 A	
	With filler material	Without filler material	With filler material	Without filler material
Cr	22.6	22.7	21.2	20.4
Ni	6.4	5.9	6.3	5.9
Mn	1.7	1.1	1.2	1.4

3.2. Analysis of the microstructure and phase ratio

After the welding tests, cross sections were made from the samples. These were taken from the locations where LIBS measurements were also taken. The LIBS measurements were only performed on the surface (i.e. at the top of the cross sections). Due to convection, it can be assumed that the surface measurements on the melt and in the solidified material is significant for the total melt volume.

Therefore, the comparison of the data with the microstructure is in order. Thus, the increased concentrations of Mn and Ni can be correlated with the phase ratio. The γ/α ratio was determined by image analysis. For this purpose, the samples were etched with the color etch Beraha II and captured with the light microscope at various locations. Figure 4 shows an example of the microstructure of an EN grade 1.4162 welded with 160 A and filler material. Overview images, detailed images of the base metal and the weld metal were taken. The microstructure shows a common appearance of a weld structure made of DSS. The base metal has a balanced phase ratio. In the weld metal, austenite precipitates at the grain boundaries, resulting in a Widmanstätten microstructure. Table 3 summarizes the ferrite contents (vol.-%) of the weld metal of the different weld configurations. The ferrite contents in the base metal were in the usual range between 50-60 vol.-% for all specimens. It is noticeable that the ferrite content decreases with filler materials. This is due to the additional Ni and Mn concentration in the filler material. Ni and Mn are austenite formers and promote the precipitation of austenite during cooling. The increased Ni and Mn concentration could be measured by the LIBS method and is also reflected in the microstructure, based on the increasing austenite contents. For EN grade 1.4462, the ferrite content is ≤ 70 vol.-%. In [26] it is required that welded joints of DSS must contain a ferrite content between 30-70 vol.-%. In contrast, the ferrite content without filler material in EN grade 1.4462 is over 90 vol.-%. The high ferrite contents lead to a degradation of the mechanical properties and a decrease in corrosion resistance. Even if the LIBS measurements with the chemical composition during welding do not correlate directly with the microstructure, correlations can be established based on the austenite formers (Ni, Mn) and the increasing austenite contents in the microstructure. The LIBS measurement can therefore be interpreted as successful and should be validated with further experiments. In further experiments, sections can also be taken from other locations of the weld seam for control purposes.



Figure 4. Exemplary image of the microstructure of a welded EN grade 1.4162, 160A with filler metal. (a) overview image of the weld; (b) image of the base metal with balanced phase ratio α/γ ; (c) detail image of the weld metal. Visible ferritization of the material.

Table 3. Ferrite volume fraction in the weld microstructure of different DSS. Volume fraction of ferrite was determined by image analysis.

Grade (EN 10088-1)		Ferrite Content (vol.-%)	
		With filler material	Without filler material
1.4162	140 A	82	89
	160 A	75	86
1.4462	140 A	69	92
	160 A	70	93

4. Conclusion

In this work, it was shown that in situ LIBS measurement can be performed during TIG welding with and without filler material of duplex stainless steels. Main results of the work are:

- Quantitative LIBS measurements of the chemical composition of duplex steels during welding could be performed.
- Mn concentrations increase during the welding process. Both, with and without filler material.
- Ni and Cr concentrations remain constant during welding. Ni concentrations, however, are increased due to the filler material.
- The ferrite contents decrease due to the increased concentration of austenite-forming elements in the weld metal (Ni, Mn).

In this work, only the influence of one parameter (filler material) on the ferrite contents was investigated. In further work, other parameters such as heat dissipation, welding current and welding speed need to be investigated. Further developments should also record the temperature during the cooling process using LIBS.

Acknowledgements

Authors would like to thank Lasertechnik Berlin GmbH (LTB) for the analytical equipment. This work was funded by the Deutsche Forschungsgemeinschaft (DFG, German Research Foundation) – 442001176.

References

- [1] Knyazeva M and Pohl M "Duplex Steels: Part I: Genesis, Formation, Structure," 2013 *Metallogr Microstruc.* **2** 113-121
- [2] Solomon H D and Devine T "Duplex Stainless Steels--A Tale of Two Phases," 1982 *Duplex stainless steels* pp. 693-756.
- [3] Knyazeva M and Pohl M "Duplex Steels. Part II: Carbides and Nitrides," 2013 *Metallography, Microstructure, and Analysis* **2** 343-351
- [4] Verma J and Taiwade R V "Effect of welding processes and conditions on the microstructure, mechanical properties and corrosion resistance of duplex stainless steel weldments-A review," 2017 *J Manuf Process* **25** 134-152
- [5] Karlsson L "Intermetallic phase precipitation in duplex stainless steels and weld metals: Metallurgy, influence on properties, welding and testing aspects," 1999 *Welding Research Council Bulletin* **438**
- [6] Karlsson L "Welding Duplex Stainless Steels — A Review Of Current Recommendations," 2012 *Welding in the World* **56** 65-76
- [7] Yang J, Wang Q, Wei Z and Guan K "Weld failure analysis of 2205 duplex stainless steel nozzle," 2014 *Case Studies in Engineering Failure Analysis* **2** 69-75
- [8] Martin G *et al.* "A macro-and micromechanics investigation of hot cracking in duplex steels," 2012 *Acta Materialia* **60** 4646-4660
- [9] Schaeffler A L "Constitution diagram for stainless steel weld metal," 1949 *Met Prog* **56** 680

- [10] Delong W T "Constitution Diagram for Stainless-Steel Weld Metal .1. Delong Diagram," 1974 *Met Prog* **106** 226-226
- [11] Kotecki D J and Siewert T A "Wrc-1992 Constitution Diagram for Stainless-Steel Weld Metals - a Modification of the Wrc-1988 Diagram," 1992 *Weld J* **71** 171-178
- [12] Kotecki D J and Rajan V B "Submerged arc fillet welds between mild steel and stainless steel," 1997 *Weld J* **76** 57-66
- [13] Wessman S "Evaluation of the WRC 1992 diagram using computational thermodynamics," 2013 *Welding in the World* **57** 305-313
- [14] Cremers D A and Radziemski L J 2006 *Handbook of laser-induced breakdown spectroscopy* vol. 2 Chichester Wiley
- [15] Collur M M, Paul A and Debroy T "Mechanism of Alloying Element Vaporization during Laser-Welding," 1987 *Metall Trans B* **18** 733-740
- [16] Khan P A A and Debroy T "Alloying Element Vaporization and Weld Pool Temperature during Laser-Welding of Aisi 202 Stainless-Steel," 1984 *Metall Trans B* **15** 641-644
- [17] Taparli U A, Jacobsen L, Griesche A, Michalik K, Mory D and Kannengiesser T "In situ laser-induced breakdown spectroscopy measurements of chemical compositions in stainless steels during tungsten inert gas welding," 2018 *Spectrochimica Acta Part B: Atomic Spectroscopy*, **139** 50-56
- [18] Taparli U A, Kannengiesser T, Cieslik K, Mory D and Griesche A "In situ chemical composition analysis of a tungsten-inert-gas austenitic stainless steel weld measured by laser-induced breakdown spectroscopy," 2020 *Spectrochimica Acta Part B: Atomic Spectroscopy* 105826
- [19] Quackatz L, Griesche A and Kannengiesser T "In situ investigation of chemical composition during TIG welding in duplex stainless steels using Laser-Induced Breakdown Spectroscopy (LIBS)," 2022 *Forces in Mechanics* **6** 100063
- [20] Mueller M, Gornushkin I B, Florek S, Mory D and Panne U "Approach to Detection in Laser-Induced Breakdown Spectroscopy," 2007 *Analytical Chemistry* **79** 4419-4426
- [21] Zhang Z M, Chen S and Liang Y Z "Baseline correction using adaptive iteratively reweighted penalized least squares," 2010 *Analyst* **135** 1138-1146
- [22] Sharaf M A, Illman D L and Kowalski B R 1986 *Chemometrics* John Wiley & Sons
- [23] R Noll 2012 *Laser-induced breakdown spectroscopy fundamentals and applications* Berlin: Springer
- [24] Zhang Y, Evans J R G and Yang S "Corrected Values for Boiling Points and Enthalpies of Vaporization of Elements in Handbooks," 2011 *Journal of Chemical & Engineering Data* **56** 328-337
- [25] Taparli U A, Kannengiesser T, Griesche A „Tungsten inert gas bead-on-plate weld chemical composition analysis by laser-induced breakdown spectroscopy,” 2020 *IOP Conference Series: Materials Science and Engineering* **882** 012023
- [26] DIN EN ISO 17781 *Erdöl-, petrochemische und Erdgasindustrie - Prüfverfahren für die Qualitätslenkung von Mikrostrukturen von ferritisch/austenitisch nichtrostenden Duplexstählen* 2017